A combined segmentation and registration framework with a nonlinear elasticity smoother

Carole Le Guyader and Luminita Vese

UCLA CAM Report 08-16, March 2008

IRMAR, UMR CNRS 6625
Institut National des Sciences Appliquées de Rennes
20 Avenue des Buttes de Coesmes CS 14315 35043 RENNES Cedex, France
cleguyad@insa-rennes.fr

UCLA Department of Mathematics
405 Hilgard Avenue
Los Angeles, CA 90095-1555, U.S.A.
lvese@math.ucla.edu

Abstract

In this paper, we present a new non-parametric combined segmentation and registration method. The problem is cast as an optimization problem combining a matching criterion similar to the one defined by the active contour without edges [6] for segmentation and a nonlinear-elasticity-based smoother on the displacement vector field. This modelling is twofold: first, in a way, registration is jointly performed with segmentation since guided by the segmentation process. It means that the algorithm produces both a smooth mapping between the two shapes and the segmentation of the object contained in the reference image. Secondly, the use of a nonlinear- elasticity-type regularizer allows large deformations to occur, which makes the model comparable in this point with the viscous fluid registration method. Several applications are proposed to demonstrate the potential of this method to both segmentation of one single image and to regisration between two images, as well as comparison tests with classical methods.

Keywords: Registration, nonlinear elasticity, Chan-Vese model for segmentation, level set method.

1 Introduction

We propose in this paper a segmentation model based on the active contour model without edges [6], that is no longer solved in terms of level set functions. This is now solved using registration techniques. Therefore, a displacement field models the deformation of the initial curve into the final segmented boundary via registration. Thus, the binary segmentation problem from [6], recalled below

$$\inf_{c_1,c_2,\phi} F(c_1,c_2,\phi) = \int_\Omega \left\{ \nu_1 |R(\mathbf{x}) - c_1|^2 H(\phi) + \nu_2 |R(\mathbf{x}) - c_2|^2 (1 - H(\phi)) + \mu |\nabla H(\phi)| \right\} d\mathbf{x}$$

(where R is the given data, ϕ is a level set function, H is the 1D Heaviside function), can be seen as a registration problem between the binary image defining the initial contour, and the (unknown) binary segmented image. Or the proposed model can also be used for registration between two images: having a segmentation of one of the images defined via a displacement field, this is used as initial guess in the "registration-segmentation" model, to segment/register the second image. The main ingredients of our proposed minimization model are thus the active contour model without edges [6], and registration via a non-linear elasticity smoother, which is solved in a particular, simplified way. We first review techniques of image registration.

1.1   Prior related work on image registration

Image registration and image segmentation are challenging issues that are encountered in a wide range of fields such as medical imaging (shape tracking, comparison of images taken at different instants, data fusion from images that have not necessarily been acquired with the same modality, comparison of data to a common frame of reference, etc...), pattern recognition or geophysics (see [2]).

Considering two images called template and reference, registration consists in finding an optimal diffeomorphic transformation (the optimality criterion being devised according to the considered application) such that the deformed template matches in some sense the reference, while segmentation aims at detecting and visualizing the contours of the objects contained in a given image.

An extensive overview of registration techniques can be found in [32] but for the sake of clarity, we briefly describe some of the possible strategies. As mentioned in [32], existing methods can be partitioned into two classes:

- parametric methods. In this case, a finite set of image features is defined and the goal is to find a transformation mapping any feature from the template image to its counterpart in the reference image. Image features can be landmarks (anatomically meaningful points, points with high-curvature, etc...), which requires the user's intervention to locate them or automatically-computed features such as principal axes (see [32], chapter 5). Also, the set of feasible transformations is restricted to a certain class of mappings (polynomial mappings, splines, etc...) by expanding the transformation in terms of basis functions.

- non-parametric methods, this class of methods being the one we are interested in. As stressed in [32], unlike parametric methods, the transformation is in this case not restricted to a parameterizable set. The problem is phrased as a functional minimization problem whose unknown is the displacement vector field u. We follow the notations of [32]. Denoting by T the template image and by R the reference, the introduced functional combines a distance measure component $\mathcal{D}[R, T, \mathbf{u}]$ and a smoother on the displacement vector field $\mathcal{S} = \mathcal{S}[\mathbf{u}]$ to remove the ill-posed character of the problem. Usually, the distance measure is intensity-driven and is chosen to be the L^2-norm of the difference between the deformed template and the reference (suitable when the images have been acquired through similar sensors) *i.e.* $\mathcal{D}[R, T, \mathbf{u}] = \dfrac{1}{2} \displaystyle\int_{\Omega} \left(T(\mathbf{x} - \mathbf{u}) - R(\mathbf{x}) \right)^2 d\mathbf{x}$, but one could also use correlation-based or mutual information-based techniques (see [32], chapter 6 for more details).

Several methods to regularize the displacement vector field have been investigated (see Part II of [32] or [17]). Generally, physical arguments motivate the way the smoothers are built. We briefly review some of them. We first consider the case of elastic registration originally introduced by Broit [5] in which the objects to be registered are considered to be the observations of a same elastic body before and after being subjected to a deformation as mentioned in [32]. The smoother $\mathcal{S} = \mathcal{S}[\mathbf{u}]$ is chosen to be the linearized elastic potential of the displacement vector field $\mathbf{u}$ and its expression integrates the Lamé coefficients which reflect material properties. It is defined, $n \in \mathbb{N}^{\star}$ being the dimension, by:

$$\mathcal{S}[\mathbf{u}] = \int_{\Omega} \frac{\mu}{4} \sum_{j,k=1}^{n} \left(\partial_{x_j} u_k + \partial_{x_k} u_j \right)^2 + \frac{\lambda}{2} \left(\mathrm{div}\ \mathbf{u} \right)^2 d\mathbf{x}.$$

A drawback of this smoother is that it is not suitable for problems involving large deformations. To circumvent this problem, Christensen and collaborators have introduced in [9] a viscous fluid registration model in which objects are viewed as fluids evolving in accordance with the fluid-dynamic Navier-Stokes equations. It consists in minimizing the linearized elastic potential of the velocity of the displacement vector field (nonlinearly related to the displacement vector field *via* the material derivative). With time, the constraint weakens as u reaches a steady state and large deformations are therefore authorized. One drawback of this method is the computational cost. Numerically, the image-related force field is first computed at time t. Fixing the force field $\mathbf{f}$, the linear PDE satisfied by the velocity is solved by means of a successive over-relaxation (SOR) scheme. Then an explicit Euler scheme is used to advance the displacement vector in time.

In the diffusion registration model introduced by Fischer and Modersitzki [15], the smoother is based on the semi-norm on $H^1(\Omega, \mathbb{R}^n)$ of $\mathbf{u} = (u_1, \cdots, u_n)^T$, Ω being an open bounded subset of $\mathbb{R}^n$ and $H^1(\Omega, \mathbb{R}^n)$ denoting the classical Sobolev space, that is:

$$\mathcal{S}[\mathbf{u}] = \frac{1}{2} \int_{\Omega} \Big[\sum_{i=1}^{n} ||\nabla u_i||^2 \Big] d\mathbf{x}.$$

Regularizing properties motivate this choice (it minimizes oscillations of both components of u) rather than physical ones but here again only small deformations can be expected in this context.

Lastly, in the "curvature"-based registration model introduced by Fischer and Modersitzki [16], [17], the smoother $\mathcal{S}$ is defined by:

$$\mathcal{S}[\mathbf{u}] = \frac{1}{2} \int_{\Omega} \Big[\sum_{i=1}^{n} (\Delta u_i)^2 \Big] d\mathbf{x}.$$

As stressed in [32], Δu_k, $k = 1, \cdots, n$ can be viewed as an approximation of the curvature so the problem boilds down to almost minimizing the "curvature" of level lines of each component of $\mathbf{u}$. Also, one can easily notice that affine linear transformations belong to the kernel of $\mathcal{S}[\mathbf{u}]$ which is not the case in elastic, viscous fluid or diffusion registration. But here again, transformations are restricted to small deformations. To circumvent this drawback, we propose in this paper, a nonlinear elasticity-based smoother as will be seen later in Section 2.

3

Many improvements or alternatives of these non-parametric methods have been proposed. We briefly shed light on some contributions in this field. In [18], Haber and Modersitzki address the issue of non-parametric image registration under volume-preserving constraints. More precisely, they propose to restrict the set of feasible mappings by adding a volume-preserving constraint which forces the Jacobian of the deformation to be equal to one.

Papers [19] and [54] are dedicated to topology-preserving constraints applied to the deformation mapping so as to keep it diffeomorphic. These methods differ from classical regridding techniques (see [10]) in which one monitors the values of the Jacobian of the deformation, stops the process when the values drop below a threshold and reinitializes the process using the deformed template obtained at the previous step.

Inspired by their previous work on volume-preserving registration [18], Haber *et al.* propose to monitor the Jacobian of the deformation in order to prevent the deformation from exhibiting twists and foldings. More precisely, the authors aim at keeping the Jacobian bounded, which leads to an inequality-constrained minimization problem. They first discretize the minimization problem and the constraints. The obtained finite dimensional optimization problem is replaced by a sequence of unconstrained optimization problems derived from the log-barrier method.

An information-theory-based approach is proposed in [54] to generate diffeomorphic mappings and to monitor the statistical distribution of the Jacobian. Assuming that the template and reference images are defined on a domain Ω whose volume is equal to 1, the authors associate a probability density function to the deformation and its inverse. Then they propose to quantify the magnitude of the deformation by means of the Kullback-Leibler distance between the probability density function associated with the deformation and the identity mapping.

Finally, some new frameworks have been studied.

In [28], the authors propose to quantify differences between images by matching gradient fields. They first define an equivalence class of images, that is, an image space in which images are considered equivalent under a similarity group action. Contrary to classical methods which involve an intensity comparison criterion and thus that are scale-dependent, the authors focus on the relative change of intensity in the images. This leads to consider a similarity group action that contains translations and rescalings. The Cauchy-Schwartz-based distance measure is then introduced. It allows to discriminate images belonging to the equivalence class from others by comparing gradient fields regardless of the scaling, this non-negative distance being zero only between equivalent images.

In [26], Liao *et al.* propose a level set-based framework for matching overlapping/non-overlapping shapes and open curves. The underlying idea is to substitute finite pairs of shapes or curves for the classical finite pairs of landmarks. The shapes and curves to be warped are modelled *via* level set functions (input in the method): a shape is represented by means of a level set function whose zero level line is the shape boundary while the representation of an open curve, borrowed from the work by Smereka [44], requires two level set functions. According to the considered case (overlapping, non-overlapping shapes, open curves), a specific distance measure is devised, coupled with a regularization on the displacement vector field $\mathbf{u}$. In the simplest case of one pair of shapes to be matched with no spatial overlap of the two shapes, denoting by φ the level set function representing the shape in the template image, Φ the one representing the shape in the reference image and $\mathbf{u}$ the sought displacement vector field, the authors propose to minimize the symmetric difference of the two level set functions,

that is:

$$\min_{\mathbf{u}} \int_{\Omega} H(\Phi(\mathbf{x}))\big[1 - H(\varphi(\mathbf{x} - \mathbf{u}))\big]\,d\mathbf{x} + \int_{\Omega} H(\varphi(\mathbf{x} - \mathbf{u}))\big[1 - H(\Phi(\mathbf{x}))\big]\,d\mathbf{x},$$

with H the one-dimensional Heaviside function. The problem is then stated in the case of one pair of shapes with spatial overlap by slightly modifying the distance measure, next extended to the case of multiple pairs of shapes and finally studied in the case of open curves.

The same kind of approach is discussed in [25] with, in addition to the modelling of open curves, the implicit representation of points. Although different, the spirit of our work is the same in the way the shapes to be registered are modelled. But unlike the model in [26], the only input required in our method is the level set function representing the template image. Also, we jointly treat segmentation and registration: the distance measure is devised using the segmentation criterion [6] while registration is jointly performed, guided by the segmentation process. Before depicting our approach, we would like to mention some previous works dedicated to joint segmentation and registration. We carefully describe two of them and stress the main differences with our model.

1.2 Prior related work on segmentation-registration

In [55], Yezzi *et al.* also suggest to jointly treat segmentation and registration. Their work is motivated by different remarks related to the interdependence between segmentation and registration processes. In landmark-based registration (also referred to as feature-based registration), ones collects a number of features in the reference image using for instance, low/high level segmentation methods and identifies their counterparts in the template image. This exemplifies the dependence that may exist of registration on segmentation. Conversely, in some fields of research such as medical imaging, *a priori* knowledge related to the geometry /shape of the organ need to be incorporated in the segmentation process. This is performed by registering the data to a common frame of reference in order to produce some statistics on the shape, geometry, etc...This highlights this time, the dependence of segmentation on registration. The focus of Yezzi *et al.*'s paper was then to provide a model, in a geometric variational framework, that interleaves segmentation and registration. In this purpose, the authors state the problem that couples segmentation and registration as follows: denoting by $I : \Omega \subset \mathbb{R}^2 \to \mathbb{R}$ and $\widehat{I} : \widehat{\Omega} \subset \mathbb{R}^2 \to \mathbb{R}$ the two images containing a common object to be registered and segmented, find a closed curve $C \subset \Omega$ and a closed curve $\widehat{C} \subset \widehat{\Omega}$ related by $\widehat{C} = \mathbf{g}(C)$ where $\mathbf{g} : \mathbb{R}^2 \to \mathbb{R}^2$ is an element of a finite dimensional group G (for instance, the group of rigid motions) such that C and $\widehat{C}$ correctly delineate the object contained respectively in I and the one contained in $\widehat{I}$. Consequently, there are two unknowns, the closed curve $C \subset \Omega$ and the mapping $\mathbf{g}$. The problem is phrased in terms of an energy minimization one. The authors exploit region-based active contour models and more precisely the piecewise constant Mumford-Shah energy inspired from [6] (see [55]) and propose to minimize the

following energy:

$$E(\mathbf{g}, C) = E_1(C) + E_2(\mathbf{g}(C)),$$

$$= \int_{C_{in}} (I - u)^2 d\mathbf{x} + \int_{C_{out}} (I - v)^2 d\mathbf{x} + \int_{\widehat{C}_{in}} (\widehat{I} - \widehat{u})^2 d\mathbf{x} + \int_{\widehat{C}_{out}} (\widehat{I} - \widehat{v})^2 d\mathbf{x},$$

$$= \int_{C_{in}} f_{in}(\mathbf{x}) d\mathbf{x} + \int_{C_{out}} f_{out}(\mathbf{x}) d\mathbf{x} + \int_{\widehat{C}_{in}} \widehat{f}_{in}(\mathbf{x}) d\mathbf{x} + \int_{\widehat{C}_{out}} \widehat{f}_{out}(\mathbf{x}) d\mathbf{x},$$

with C_{in} and C_{out} the regions inside and outside C, u and v the mean values of I on C_{in} and C_{out} and with $\widehat{C}_{in}$ and $\widehat{C}_{out}$ the regions inside and outside $\widehat{C}$, $\widehat{u}$ and $\widehat{v}$ the mean values of I on $\widehat{C}_{in}$ and $\widehat{C}_{out}$. The constraint enforced on $\widehat{C}$, namely $\widehat{C} = \mathbf{g}(C)$ enables us to rewrite the energy E using only integrals over the domain Ω as:

$$E(\mathbf{g}, C) = \int_{C_{in}} \left(f_{in}(\mathbf{x}) + \widehat{f_{in}}(\mathbf{g}(\mathbf{x}))|\mathbf{g}'(x)| \right) d\mathbf{x} + \int_{C_{out}} \left(f_{out}(\mathbf{x}) + \widehat{f_{out}}(\mathbf{g}(\mathbf{x}))|\mathbf{g}'(\mathbf{x})| \right) d\mathbf{x},$$

$|\mathbf{g}'|$ being the Jacobian of $\mathbf{g}$. As stressed by the authors, both contours are jointly deformed, which guarantees same detected shapes and segmentation - registration are simultaneously performed. A weighted combination of the energies E_1 and E_2 could be considered in case segmentation on one image is harder to perform. Also, a more complex energy could be built in order to let the unknown $\mathbf{g}$ be more influenced by the energy E_1. It would mainly consist in assuming that the unknown curve C lives in a domain different from Ω and in considering two mappings $\mathbf{g_1} \in G$ and $\mathbf{g_2} \in G$: one to map C to Ω and the other one to map $\widehat{C}$ to $\widehat{\Omega}$. A gradient descent method is applied, which yields the evolution equations of C and of the registration parameters. The main difference with our model is that the contours C and $\widehat{C}$ are jointly deformed here through a combination of segmentation and registration methods while in our model, we assume that the object in the template image has already been detected (we could have considered a problem with two unknowns as well). It means that the energy-minimization problem is only written in terms of the unknown contour $\widehat{C}$. Segmentation is performed using a registration approach as in [55]. The model is cast in the level set setting, which allows a straightforward modelling of the evolving curve. At last, contrary to [55], the class of admissible deformations (rigid, etc...) is not an input in our model. Their model, first exposed in the context of rigid deformations, has then been extended to non-rigid motions (see [52], [51] or [46]).

We would like also to mention the very interesting work by Lord *et al.* which uses a matching criterion based on metric structure comparison. In [29], Lord *et al.* address the issue of quantifying differences between homologous shapes. Their work comes within the context of hippocampi shape analysis and is motivated by the fact that disease classification is made easier after having compared regional asymmetries. In order to perform this comparative analysis, the authors propose a unified method that simultaneously treats segmentation and registration by introducing two unknowns in the process: the deformation map and the segmenting curve. The segmentation process is guided by the registration map and the matching criterion, unlike classical registration methods, rests on the metric structure comparison of both surfaces and more precisely on the minimization of deviation from isometry. Indeed, to devise their model, the authors formulate some fundamental assumptions: first, "the deformity of homologous anatomical structures can be quantified as the deviation from

isometry of the deformation map between their surfaces". Second, "since deformities may be local, the evolution of the global correspondence must allow for a partial disconnection between the normal and abnormal regions." Several ingredients from differential geometry are required to cast the model in a computational framework similar to the one of 2D image segmentation and registration. To begin with, the authors use the argument according to which any zero-genus closed shape is topologically equivalent to the sphere. Thus hippocampi can be viewed as 2D Riemannian manifolds embedded in $\mathbb{R}^3$ topologically equivalent to the sphere. By excluding two poles, one gets a surface topologically equivalent to the cylinder, which allows to parameterize it on a rectangular domain (equipped with periodic boundary conditions). Consequently, this approach enables the authors to define the integrals involved in the objective functional on the rectangular domain P_1 related to the surface S_1. The matching criterion introduced is based on the metric structure comparison of the surfaces, more precisely on their first fundamental form (FFF), and on a Chan-Vese-like homogeneity constraint. The first fundamental form encodes intrinsic geometric properties of a surface, the term 'intrinsic' meaning that no appeal to the ambient space is required. As mentioned in [12] [Section 2.5 page 92], denoting by $S \subset \mathbb{R}^3$ the surface, T_pS the tangent plane at $p \in S$ of the regular surface S, the FFF is defined as the quadratic form $I_p : \begin{array}{l} T_pS \to \mathbb{R} \\ \mathbf{w} \mapsto < \mathbf{w}, \mathbf{w} >_p = |\mathbf{w}|^2 \geq 0 \end{array}$, $< \mathbf{w_1}, \mathbf{w_2} >_p$ with $\mathbf{w_1}, \mathbf{w_2} \in T_pS \times T_pS$ denoting the inner product of $\mathbf{w_1}$ and $\mathbf{w_2}$ as vectors in $\mathbb{R}^3$.

Assuming that the surface S is determined by $\mathbf{x}(u,v)$ and denoting by $\mathbf{x}_u = \dfrac{\partial \mathbf{x}}{\partial u}$ and $\mathbf{x}_v = \dfrac{\partial \mathbf{x}}{\partial v}$, the matrix representation of the FFF in the basis $\{\mathbf{x}_u, \mathbf{x}_v\}$ is given by $\begin{pmatrix} E & F \\ F & G \end{pmatrix}$ with $\begin{cases} E = <\mathbf{x}_u, \mathbf{x}_u> \\ F = <\mathbf{x}_u, \mathbf{x}_v> \\ G = <\mathbf{x}_v, \mathbf{x}_v> \end{cases}$.

The FFF is related to the intrinsic geometry of the surface and some local properties (lengths, areas) can be computed only in terms of E, F and G. The "element of arclength" (also referred to as induced Riemannian metric) is defined by $ds^2 = Edu^2 + 2Fdudv + Gdv^2$ and the element of area is defined by $dA = ||\mathbf{x}_u \times \mathbf{x}_v||dudv = \sqrt{EG - F^2}dudv$.

Lastly, to compare the metric structures of the surfaces and more precisely to minimize the deviation from isometry, the authors use the fact that an isometry between two surfaces preserves the first fundamental form. The problem thus boils down to the comparison of two matrices as will be seen later. We use the same notations as in [29]. Let S_1 and S_2 be the two considered homologous surfaces, P_1 and P_2 their respective rectangular domain of parametrization and $\gamma_1 \subset S_1$, $\gamma_2 \subset S_2$ sets of closed curves. Let $\mathbf{x}(u,v)$ with $(u,v) \in P_1$ determine S_1 and $\widehat{\mathbf{x}}(\widehat{u}, \widehat{v})$ with $(\widehat{u}, \widehat{v}) \in P_2$ determine S_2. Lord $et\ al.$'s goal is to find a homeomorphic map $\mathbf{f}$ of P_1 onto P_2 - $\mathbf{f} : \begin{array}{l} P_1 \to P_2 \\ (u,v) \mapsto (\widehat{u}, \widehat{v}) = \mathbf{f}(u,v) \end{array}$ -(diffeomorphic except possibly on the curves γ) to register S_1 and S_2 and a segmenting curve γ_1 such that γ_1 delineates regions in S_1 and its counterpart γ_2, regions of S_2. The FFF matrix associated to S_1 is denoted by G_1, $\left(G_1 = \begin{pmatrix} <\mathbf{x}_u, \mathbf{x}_u> & <\mathbf{x}_u, \mathbf{x}_v> \\ <\mathbf{x}_u, \mathbf{x}_v> & <\mathbf{x}_v, \mathbf{x}_v> \end{pmatrix}\right)$ and the one associated to S_2 is denoted by G_2, $\left(G_2 = \begin{pmatrix} <\widehat{\mathbf{x}}_{\widehat{u}}, \widehat{\mathbf{x}}_{\widehat{u}}> & <\widehat{\mathbf{x}}_{\widehat{u}}, \widehat{\mathbf{x}}_{\widehat{v}}> \\ <\widehat{\mathbf{x}}_{\widehat{u}}, \widehat{\mathbf{x}}_{\widehat{v}}> & <\widehat{\mathbf{x}}_{\widehat{v}}, \widehat{\mathbf{x}}_{\widehat{v}}> \end{pmatrix}\right)$.

Denoting by J the Jacobian matrix of $\mathbf{f}$, $\left(J = \begin{pmatrix} \dfrac{\partial f_1}{\partial u} & \dfrac{\partial f_1}{\partial v} \\ \dfrac{\partial f_2}{\partial u} & \dfrac{\partial f_2}{\partial v} \end{pmatrix} \right)$, one can easily check that the FFF matrix related to S_2 parameterized by $\begin{array}{c} P_1 \to \mathbb{R}^3 \\ (u,v) \mapsto \widehat{x} \circ \mathbf{f}(u,v) \end{array}$ is defined by $J^T G_2 J$. The matching criterion resting on the measure of deviation from isometry, the authors propose to minimize the distance between G_1 and $J^T G_2 J$ by means of the Frobenius norm since an isometry preserves the first fundamental form. Also, a Chan-Vese-like homogeneity constraint is enforced in the objective functional. The region of S_1 inside the curve γ_1 exhibits one kind of deformation while the region outside shows another. Thus contrary to our model in which the expected curve (implicitly represented as the zero level set of a Lipschitz function) delineates two regions with homogeneous intensity , their criterion is still based on metric structure comparisons to disconnect normal regions from abnormal ones.

To conclude this section, we would like to mention the related work by Vemuri $et\ al.$ [48], [49]. The authors propose a coupled PDE model to perform both segmentation and registration. In the first PDE, the level sets of the source image are evolved along their normals with a speed defined as the difference between the target and the evolving source image. The second PDE allows to explicitly retrieve the displacement vector field. In particular, in the work of Vemuri-Chen [47] for joint registration and segmentation, the piecewise-smooth level set segmentation model from [50] is combined with prior shape information through global alignment, by minimizing the energy

$$E(\phi, u^+, u^-, \mu, R, T) = \alpha \int_\Omega |u^+ - I|^2 H(\phi) d\mathbf{x} + \alpha \int_\Omega |u^- - I|^2 (1 - H(\phi)) d\mathbf{x}$$

$$+ \beta \int_\Omega |\nabla u^+|^2 H(\phi) d\mathbf{x} + \beta_\Omega |\nabla u^-|^2 (1 - H(\phi)) d\mathbf{x} + \int_\Omega d^2(\mu R \mathbf{x} + T)\delta(\phi)|\nabla \phi| d\mathbf{x},$$

where I is the given image to be segmented, ϕ the unknown level set function, μ is a scale, R is rotation, T is translation, and d is the given distance function defined from the prior shape. As we will see below, our model is different from the one in [47]. For the sake of completeness, we also refer the reader to [8] in which a geodesic-active-contour-based model including a shape prior is presented and [7] in which a shape prior is incorporated this time in the Mumford-Shah model.

Related work is presented in [14], on an atlas-based segmentation of medical images locally constrained by level sets. Finally, we wish to refer to a segmentation method, different from ours, that also uses nonlinear elasticity to define the deformation of the evolving contour or surface in Rouchdy et al. [40]. The segmentation criteria is based on the gradient vector flow [53], and a deformation field is computed via non-linear elasticity using the finite element method.

We now present our model. The outline of the paper is as follows: section 2 is devoted to the depiction of our model. We carefully comment on the way the functional minimization problem is defined. In section 3, the algorithm is detailed and numerical experiments are given in order to demonstrate the potential of this method.

2 Description of the proposed model

As mentioned in the introduction, the scope of the proposed method is twofold:

- we want to devise a model in which segmentation and registration are jointly performed.

- large and smooth deformations must be authorized while keeping the deformation map diffeomorphic.

We see in the sequel how these criteria are fulfilled.

2.1 Distance measure criterion

Let Ω be a bounded open subset of $\mathbb{R}^n$. For the purpose of illustration, we consider the case $n = 2$.

Let us denote by $R : \bar{\Omega} \to \mathbb{R}$ the "reference" image to be segmented (later we will discuss how the proposed method can be used for registration between a template image $T : \bar{\Omega} \to \mathbb{R}$ and the reference image R). But originally, our method is defined as a segmentation method based on [6], recalled in the introduction. Let Φ_0 be a given Lipschitz level set function. Denoting by $\mathcal{C}$ the zero level set of Φ_0 and $w \subset \Omega$ the open set it delineates, Φ_0 is such that:

$$\begin{cases} \mathcal{C} = \big\{ \mathbf{x} \in \Omega \mid \Phi_0(\mathbf{x}) = 0 \big\} \\ w = \big\{ \mathbf{x} \in \Omega \mid \Phi_0(\mathbf{x}) > 0 \big\} \\ \Omega - \bar{w} = \big\{ \mathbf{x} \in \Omega \mid \Phi_0(\mathbf{x}) < 0 \big\}. \end{cases}$$

The deformaton of the evolving curve is made in order to satisfy a segmentation criterion. Indeed, the distance measure we introduce is related to the fitting term in the segmentation [6]. We recall that this method is a particular case of the minimal partition problem. Contrary to classical methods which involve a stopping criterion based on the image gradient, this method is region-based and aims at finding the best partition of the image as a function taking only two values. By this way, registration and segmentation are correlated and we expect at the end of the process to obtain the segmentation of the reference image as well as a smooth deformation map. It results in a region-based intensity approach and no longer in a pointwise process as usually done. The idea is to find a smooth displacement vector field $\mathbf{u} : \begin{array}{l} \Omega \to \mathbb{R}^2 \\ \mathbf{x} \mapsto (u_1(\mathbf{x}), u_2(\mathbf{x})) \end{array}$ such that the zero level line of Φ defined by $\Phi(\mathbf{x}) = \Phi_0(\mathbf{x} - \mathbf{u}(\mathbf{x}))$ fits the boundary of the object to be warped in the given "reference" image. Denoting by H the one-dimensional Heaviside function, by $\nu_1, \nu_2 > 0$ two fixed parameters and c_1 and c_2 being two unknown constants depending on Φ_0 and $\mathbf{u}$, the distance measure functional F_d (the segmentation criteria) is defined by:

$$F_d(c_1, c_2, \mathbf{u}) = \nu_1 \int_\Omega |R(\mathbf{x}) - c_1|^2 H\big(\Phi_0(\mathbf{x} - \mathbf{u}(\mathbf{x}))\big) \; d\mathbf{x}$$

$$+ \nu_2 \int_\Omega |R(\mathbf{x}) - c_2|^2 \Big(1 - H\big(\Phi_0(\mathbf{x} - \mathbf{u}(\mathbf{x}))\big) \Big) \; d\mathbf{x}. \tag{1}$$

We need to add a regularization term of the form $F_{reg}(\mathbf{u})$ to (1), which is a substitute for the length term of the evolving curve in [6], and therefore the unknown $\Phi(\mathbf{x})$ from [6] is substituted by $\Phi_0(\mathbf{x} - \mathbf{u}(\mathbf{x}))$, with Φ_0 fixed now. Thus, we obtain a binary segmentation method that can also be used for registration.

2.2 Introduction of a nonlinear elasticity-based regularizer

A regularizing term F_{reg} is now introduced to ensure the smoothness of the displacement vector field u. As stressed by Fischer and Modersitzki [17], the smoother depends on the particular properties required for the displacement vector field and is related to the physics of the object under consideration. To allow large deformations, we introduce a nonlinear-elasticity-based smoother. For completeness, we also refer the reader to [4], [31] for a variational form registration method for large deformations, and to [39], a much related work which also uses nonlinear elasticity regularization but which is implemented using the finite element method.

We propose to view the deformation of the initial contour into the final segmented contour as the deformation undergone by St. Venant-Kirchhoff materials. These materials are homogeneous, isotropic, hyperelastic and the axiom of frame indifference is satisfied (see [11] for further details). Let us denote by ϵ the Green-St. Venant strain tensor defined by: $\epsilon = \frac{1}{2}(C - I)$ with $C = \nabla\varphi^T \nabla\varphi$, φ being the deformation such that $\varphi = \mathbf{Id} + \mathbf{u}$, $\nabla\varphi$ being the Jacobian matrix and I denoting the identity matrix. We have equivalently $\epsilon = \epsilon(\mathbf{u}) = \frac{1}{2}(\nabla\mathbf{u}^T + \nabla\mathbf{u} + \nabla\mathbf{u}^T\nabla\mathbf{u})$. The strain tensor is a measure of the deviation between a given deformation and a rigid deformation for which $C = I$. As stressed by Ciarlet [11], St. Venant-Kirchhoff materials are the simplest among nonlinear models: they obey the simplest constitutive equation, that is their response functions are given by $\Sigma(\epsilon) = \lambda \mathrm{tr}\epsilon\, I + 2\mu\epsilon$, λ and μ being the Lamé constants. Their stored energy function is given by $W(\epsilon) = \frac{\lambda}{2}(\mathrm{tr}\epsilon)^2 + \mu\mathrm{tr}\epsilon^2$. Setting $C = F^T F$, the stored energy W can be rewritten in the form (see [11] for details):

$$\widehat{W}(F) = W(\epsilon) = -\frac{3\lambda + 2\mu}{4}\mathrm{tr}C + \frac{\lambda + 2\mu}{8}\mathrm{tr}C^2 + \frac{\lambda}{4}\mathrm{tr}\,\mathrm{Cof}\,C + \frac{6\mu + 9\lambda}{8}. \tag{2}$$

Raoult [23] (see also [38]) proved that the stored energy function of a St. Venant-Kirchhoff material is not polyconvex. It is also not rank-1 convex and consequently not quasiconvex, which raises a drawback of theoretical nature since we cannot obtain weak lower semi-continuity of the introduced functional. Also, as stressed by Ciarlet in [11], the stored energy lacks a term preventing the Jacobian matrix of φ to approach zero.

Nevertheless, despite all these underlying hindrances, we can expect to get better results than those obtained with linearized models, as will be demonstrated in the following. The nonlinear elasticity regularizer that will be coupled with the distance measure functional F_d is defined by:

$$F_{reg}(\mathbf{u}) = \int_\Omega W(\epsilon(\mathbf{u}))\,d\mathbf{x} = \int_\Omega \left\{\frac{\lambda}{2}(\mathrm{tr}\epsilon(\mathbf{u}))^2 + \mu\mathrm{tr}\epsilon^2(\mathbf{u})\right\}d\mathbf{x}. \tag{3}$$

The computation of the Euler-Lagrange equation satisfied by $\mathbf{u}$ is cumbersome. Following the idea of the more theoretical work [34], we propose to circumvent this issue by introducing a second unknown, a matrix variable V, which approximates the Jacobian matrix of $\mathbf{u}$. The nonlinear elasticity regularizer is thus applied to V and no longer to $\nabla\mathbf{u}$, that is, the nonlinearity is no longer in the derivatives of the unknown $\mathbf{u}$. Also, as the matrix variable V is introduced to mimic the Jacobian matrix of $\mathbf{u}$, an additional term based on the Frobenius norm denoted $||\cdot||_F$ of $\nabla\mathbf{u} - V$ is incorporated in the modelling. More precisely, letting $\widehat{V} = \frac{V^T + V + V^T V}{2}$ and $\alpha > 0$ a tuning parameter, we redefine the smoothing functional $F_{reg} = F_{reg}(\mathbf{u}, V)$ by:

$$F_{reg}(\mathbf{u}, V) = \int_\Omega W(\widehat{V})\,d\mathbf{x} + \frac{\alpha}{2}\int_\Omega ||\nabla\mathbf{u} - V||_F^2\,d\mathbf{x}. \tag{4}$$

In the limit, as $\alpha \to +\infty$, we obtain $\nabla \mathbf{u} \simeq V$ in the L^2-topology.

2.3 Total energy functional

The total energy E_{total} considered in the remainder of this work is given by:

$$E_{total}(c_1, c_2, \mathbf{u}, V) = F_d(c_1, c_2, \mathbf{u}) + F_{reg}(\mathbf{u}, V). \tag{5}$$

3 Implementation and numerical simulations

3.1 Evolution problem

In the sequel, we give the details of the derivation of the Euler-Lagrange equations in the two-dimensional case. In the calculations, the Heaviside function being not differentiable, it is replaced by a smooth version denoted by H_ϵ and $H'_\epsilon = \delta_\epsilon$, regularization of the Dirac measure. Fixing $\mathbf{u}$ and V and minimizing $E_{total}(c_1, c_2, \mathbf{u}, V)$ with respect to c_1 and c_2 yields:

$$c_1 = \frac{\int_\Omega R(\mathbf{x}) H\big(\Phi_0(\mathbf{x} - \mathbf{u}(\mathbf{x}))\big) \, d\mathbf{x}}{\int_\Omega H\big(\Phi_0(\mathbf{x} - \mathbf{u}(\mathbf{x}))\big) \, d\mathbf{x}}, \tag{6}$$

$$c_2 = \frac{\int_\Omega R(\mathbf{x}) \Big(1 - H\big(\Phi_0(\mathbf{x} - \mathbf{u}(\mathbf{x}))\big)\Big) \, d\mathbf{x}}{\int_\Omega \Big(1 - H\big(\Phi_0(\mathbf{x} - \mathbf{u}(\mathbf{x}))\big)\Big) \, d\mathbf{x}}. \tag{7}$$

Computing the first variation of functional $F_d(c_1, c_2, \mathbf{u})$ in (1) with respect to $\mathbf{u}$ gives the following gradient:

$$\partial_\mathbf{u} F_d(c_1, c_2, \mathbf{u}) = \big(\nu_2 (R - c_2)^2 - \nu_1 (R - c_1)^2\big) \delta_\epsilon \big(\Phi_0(\mathbf{x} - \mathbf{u}(\mathbf{x}))\big) \nabla \Phi_0(\mathbf{x} - \mathbf{u}(\mathbf{x})). \tag{8}$$

Also, computing the first variation of functional $F_{reg}(\mathbf{u}, V)$ in equation (4) with respect to $\mathbf{u}$ gives:

$$\partial_{u_k} F_{reg}(\mathbf{u}, V) = -\alpha \left(\Delta u_k - \Big(\frac{\partial v_{k1}}{\partial x_1} + \frac{\partial v_{k2}}{\partial x_2}\Big) \right), \quad k = 1, 2. \tag{9}$$

To finish, setting $V = (v_{ij})_{1 \leq i,j \leq 2}$ and letting

$$\left|\begin{aligned} & c_{01} = v_{11} + v_{22} + \tfrac{1}{2}\big(v_{11}^2 + v_{12}^2 + v_{21}^2 + v_{22}^2\big) \\ & c_{02} = 2v_{11} + v_{11}^2 + v_{21}^2 \\ & c_{03} = 2v_{22} + v_{12}^2 + v_{22}^2 \\ & c_{04} = v_{12} + v_{21} + v_{11}v_{12} + v_{21}v_{22}, \end{aligned}\right.$$

we obtain:

$$\partial_{v_{11}} F_{reg}(\mathbf{u}, V) = \alpha\big(v_{11} - \frac{\partial u_1}{\partial x_1}\big) + (\lambda c_{01} + \mu c_{02})(1 + v_{11}) + \mu c_{04} v_{12}.$$

$$\partial_{v_{12}} F_{reg}(\mathbf{u}, V) = \alpha\big(v_{12} - \frac{\partial u_1}{\partial x_2}\big) + (\lambda c_{01} + \mu c_{03}) v_{12} + \mu c_{04}(1 + v_{11}).$$

$$\partial_{v_{21}} F_{reg}(\mathbf{u}, V) = \alpha\big(v_{21} - \frac{\partial u_2}{\partial x_1}\big) + (\lambda c_{01} + \mu c_{02}) v_{21} + \mu c_{04}(1 + v_{22}).$$

$$\partial_{v_{22}} F_{reg}(\mathbf{u}, V) = \alpha\big(v_{22} - \frac{\partial u_2}{\partial x_2}\big) + (\lambda c_{01} + \mu c_{03})(1 + v_{22}) + \mu c_{04} v_{21}. \tag{10}$$

We solve the Euler-Lagrange equations in $\mathbf{u}$ and V using the gradient descent method, parameterizing the gradient descent direction by an artificial time $t \geq 0$.

$$\frac{\partial V}{\partial t} = -\partial_V F_{reg}(\mathbf{u}, V), \tag{11}$$

$$\frac{\partial \mathbf{u}}{\partial t} = -\partial_{\mathbf{u}} F_d(c_1, c_2, \mathbf{u}) - \partial_{\mathbf{u}} F_{reg}(\mathbf{u}, V), \tag{12}$$

which gives systems of 4 and 2 equations respectively, equipped with the necessary boundary conditions originally from the computation of the Euler-Lagrange equations and the initial conditions: $\mathbf{u}(x, 0) = 0_{\mathbb{R}^2}$ and $V = 0_{M_2(\mathbb{R})}$.

3.2   Implementation and algorithm

Let Δx_1 and Δx_2 be the spatial steps, Δt be the time step and $(x_{1i}, x_{2j}) = (i\Delta x_1, j\Delta x_2)$ be the grid points , $1 \leq i \leq M$ and $1 \leq j \leq N$. For a function $\Psi : \Omega \to \mathbb{R}$, let $\Psi_{ij}^n = \Psi(i\Delta x_1, j\Delta x_2, n\Delta t)$. We define the following finite difference schemes:

$$D^{x_1} \Psi_{i,j}^n = \frac{\Psi_{i+1,j}^n - \Psi_{i-1,j}^n}{2\Delta x_1} \qquad D^{x_2} \Psi_{i,j}^n = \frac{\Psi_{i,j+1}^n - \Psi_{i,j-1}^n}{2\Delta x_2}$$

$$D^{x_1 x_1} \Psi_{i,j}^n = \frac{\Psi_{i+1,j}^n - 2\Psi_{i,j}^{n+1} + \Psi_{i-1,j}^n}{\Delta x_1^2} \qquad D^{x_2 x_2} \Psi_{i,j}^n = \frac{\Psi_{i,j+1}^n - 2\Psi_{i,j}^{n+1} + \Psi_{i,j-1}^n}{\Delta x_2^2}.$$

In the following, for the sake of simplicity, we will use the notations $\Psi^n := \Psi_{i,j}^n$, $D^{x_l} \Psi^n := D^{x_l} \Psi_{i,j}^n$, $D^{x_l x_l} \Psi^n := D^{x_l x_l} \Psi_{i,j}^n$, $l = 1, 2$.

To discretize (11), we use a semi-implicit finite difference scheme as follows:

$$\frac{v_{11}^{n+1} - v_{11}^n}{\Delta t} = \alpha\big(D^{x_1} u_1^n - v_{11}^{n+1}\big) - (\lambda c_{01}^n + \mu c_{02}^n)(1 + v_{11}^n) - \mu c_{04}^n v_{12}^n,$$

$$\frac{v_{12}^{n+1} - v_{12}^n}{\Delta t} = \alpha\big(D^{x_2} u_1^n - v_{12}^{n+1}\big) - (\lambda c_{01}^n + \mu c_{03}^n) v_{12}^n - \mu c_{04}^n (1 + v_{11}^n),$$

$$\frac{v_{21}^{n+1} - v_{21}^n}{\Delta t} = \alpha\big(D^{x_1} u_2^n - v_{21}^{n+1}\big) - (\lambda c_{01}^n + \mu c_{02}^n) v_{21}^n - \mu c_{04}^n (1 + v_{22}^n),$$

$$\frac{v_{22}^{n+1} - v_{22}^n}{\Delta t} = \alpha\big(D^{x_2} u_2^n - v_{22}^{n+1}\big) - (\lambda c_{01}^n + \mu c_{03}^n)(1 + v_{22}^n) - \mu c_{04}^n v_{21}^n. \tag{13}$$

12

In a similar way, we use a semi-implicit finite difference scheme to discretize (12):

$$\frac{u_1^{n+1} - u_1^n}{\Delta t} = \big(\nu_1(R - c_1^n)^2 - \nu_2(R - c_2^n)^2\big)\delta_\epsilon\big(\Phi_0(\mathbf{x} - \mathbf{u}^n(\mathbf{x}))\big)\frac{\partial \Phi_0^n}{\partial x_1}(\mathbf{x} - \mathbf{u}^n(\mathbf{x}))$$

$$+ \alpha\bigg(D^{x_1 x_1} u_1^n + D^{x_2 x_2} u_1^n - \big(D^{x_1} v_{11}^n + D^{x_2} v_{12}^n\big)\bigg),$$

$$\frac{u_2^{n+1} - u_2^n}{\Delta t} = \big(\nu_1(R - c_1^n)^2 - \nu_2(R - c_2^n)^2\big)\delta_\epsilon\big(\Phi_0(\mathbf{x} - \mathbf{u}^n(\mathbf{x}))\big)\frac{\partial \Phi_0^n}{\partial x_2}(\mathbf{x} - \mathbf{u}^n(\mathbf{x}))$$

$$+ \alpha\bigg(D^{x_1 x_1} u_2^n + D^{x_2 x_2} u_2^n - \big(D^{x_1} v_{21}^n + D^{x_2} v_{22}^n\big)\bigg). \tag{14}$$

In most cases, no regridding was necessary. Nevertheless, in the algorithm, we have used a regridding technique quite similar to the one proposed by Christensen *et al.* [10]. The Jacobian $|\nabla\mathbf{u}| := \det(\nabla\mathbf{u})$ is monitored and if it drops below a defined threshold in some parts of the image, the process is reinitialized (necessary only when we wish to preserve the topology of the evolving contour). The only change is that instead of doing the reinitialization step with the last deformed template as done in [10], we use the last deformed level set function $\Phi_0(\cdot - \mathbf{u}(\cdot))$. The overall displacement vector field $\mathbf{u}$ is reconstructed similarly to [10]. The algorithm can be summarized as follows:

Algorithm 1 Combined segmentation and registration framework with nonlinear elasticity smoother

---

1: Read image R and define Φ_0. Initialize $n = 0$, $t = 0$, $\mathbf{u}(\mathbf{x}, 0) = 0_{\mathbb{R}^2}$, $V(\mathbf{x}, 0) = 0_{M_2(\mathbb{R})}$, flag $= 1$.

2: Compute c_1 and c_2 using relations (6) and (7).

3: Calculate $V(\mathbf{x}, n\Delta t)$ and $\mathbf{u}(\mathbf{x}, n\Delta t)$ using the semi-implicit schemes (13) and (14). $V(\mathbf{x}, n\Delta t)$ and $\mathbf{u}(\mathbf{x}, n\Delta t)$ are jointly computed, which means that $\mathbf{u}(\mathbf{x}, n\Delta t)$ is computed using updated values of $V(\cdot, n\Delta t)$.

4: Compute $|\nabla\mathbf{u}|$. If there exists $(i, j) \in [1, M] \times [1, N]$ such that $|\nabla\mathbf{u}|_{i,j} < $ tol then set flag $= 0$ and $\Phi_0 := \Phi_0(\cdot - \mathbf{u}(\cdot))$. Save the last computed displacement vector field $\mathbf{u}^{n-1}$, reinitialize $\mathbf{u}(\mathbf{x}, n\Delta t) = 0_{\mathbb{R}^2}$, $V(\mathbf{x}, n\Delta t) = 0_{M_2(\mathbb{R})}$ and go to step 2.

5: If the cost functional E_{total} decreases by sufficiently small amount compared to the previous iteration, then if flag $= 0$ compute the global displacement vector field $\mathbf{u}$ and stop else stop.

6: Let $n := n + 1$ and go to step 2.

3.3 Numerical experiments

We conclude this paper by presenting several results and comparisons on both synthetic and real images in 2 dimensions. The experiments have been performed on a 2.21GHz Athlon with 1.00 GB of RAM. In all our experiments, $\Delta x_1 = \Delta x_2 = 1$, $\nu_1 = \nu_2 = 1$ and the $\mathcal{C}^\infty$ regularization of the Heaviside funtion (see [6]) is $H_\epsilon(z) = \frac{1}{2}\big(1 + \frac{2}{\pi}\arctan\frac{z}{\epsilon}\big)$. Our first experimental test is an academic one and is similar to those performed by Modersitzki in [32] (pp 114-115, pp 129-130, pp 150-153, pp 168-170). The problem is to warp a black disk to the letter C both defined on the same image domain (size 80×80). The given data

are the template and reference images as well as the curve delineating the disk boundary. We wish to demonstrate that our method qualitatively performs in a way similar to the fluid model without requiring the expensive Navier-Stokes solver employed for its numerical discretization and provides two results: the segmentation of the reference image as well as a smooth diffeomorphic displacement vector field $\mathbf{u}$. The implementation is simple, based on finite difference schemes as previously depicted, and allows to remove the nonlinearity in the derivatives of the unknown $\mathbf{u}$. The method allows large deformations unlike the linear elasticity model, diffusion model, curvature-based model for which the registration cannot be accomplished, the images differing too much (see pages 114-115, 150-153, 168-171 from [32]). In this example, two regridding steps were necessary: the transformation was considered as admissible if the Jacobian exceeded 0.03. Note that regridding steps were also necessary with the fluid registration model.

The second example illustrates how the method can be used in the case of topology-preserving segmentation (see [1], [20], [21], [24], [45] for instance, for this topic). This synthetic reference image represents two disks (similar to tests performed in prior related works by Han *et al.* [21] and by Sundaramoorthi and Yezzi [45]). The template image, defined on the same image domain (size 100×100) is made of a black ellipse such that, when superimposed on the reference image, its boundary encloses the two disks. We aim at segmenting these two disks while maintaining the same topology throughout the process (one path-connected component) and at obtaining a smooth displacement vector field $\mathbf{u}$. In this example, one regridding step was necessary: the transformation was considered as admissible if the Jacobian exceeded 0.03.

The method has been tested on complex slices of the brain. The goal is to register a disk to a slice of the brain. The template image, defined on the same image domain (size 128×192) is made of a disk such that, when superimposed on the reference image, its boundary encloses the slice of the brain. In this example, one regridding step was necessary: the transformation was considered as admissible if the Jacobian exceeded 0.03.

4   Conclusion

This paper was devoted to a combined segmentation and registration framework allowing large deformations. The proposed variational model is based on a nonlinear elasticity regularizer and a distance measure related to the Chan-Vese model for segmentation. Contrary to prior works on nonlinear elasticity using the finite element method, the implementation is made introducing a second unknown that mimics the Jacobian matrix of the displacement vector field $\mathbf{u}$, thus removing the nonlinearity on the derivatives of $\mathbf{u}$ and decreasing the computational cost. The method produces both the segmentation of the object contained in the reference image and a smooth deformation between the template and reference images. For experiments requiring relatively large deformations, in most cases, no regridding step is necessary. For extreme cases such as the warping of the black disk to the letter C, only a few regridding steps ($\simeq 2$) is required. We also demonstrated how this method could be used in the case of topology-preserving segmentation.

In the future, we plan to investigate other topology-preserving techniques to ensure that the deformation is diffeomorphic and extend our model to piecewise-constant images with more than two intensities or textured images. Also, we are currently working on a model in which the shapes to be registered are viewed as Ogden materials. In this case, theoretical results on the existence of minimizers can be obtained.
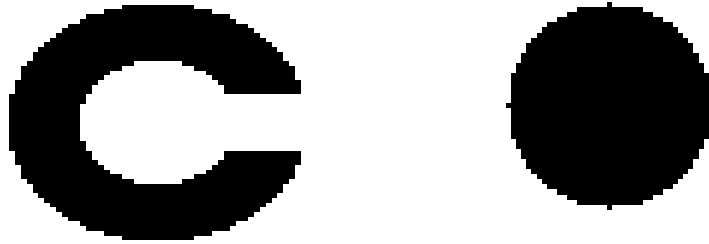
Figure 1: On the left, the reference image, on the right the template.
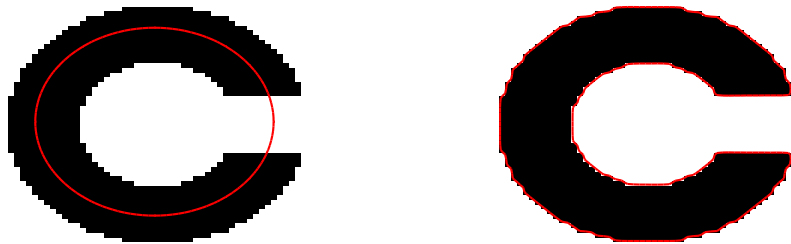
Figure 2: On the left, the boundary of the disk (zero level set of Φ_0) superimposed on the reference image, on the right the segmentation of the letter C.
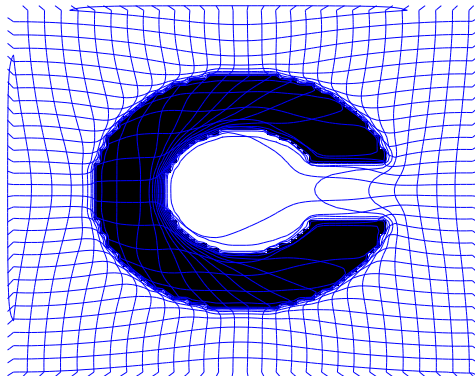
Figure 3: Deformed grid using nonlinear elasticity regularization. The parameters are: $\Delta t = 0.01$, Lamé coefficients $\lambda = 0$ and $\mu = 1000$, $\alpha = 20000$.

References

[1] O. Alexandrov and F. Santosa. A topology-preserving level set method for shape optimization. *Journal of Computational Physics*, 204(1):121–130, 2005.

[2] D. Apprato, J.-B. Betbeder, C. Gout, and S. Vieira-Testé. A Segmentation Method under Geometrical Constraints After Pre-Processing. *Curves and Surfaces IV, A. Cohen, C. Rabut, L. L. Schumaker eds.*, pages 9–18, 2000.

[3] G. Aubert and P. Kornprobst. *Mathematical Problems in Image processing: Partial Differential Equations and the calculus of Variations*. Springer Verlag, 2002.

[4] F. Beg, M. Miller, A. Trouvé, and L. Younes. Computing large deformation metric mappings via geodesic flows of diffeomorphisms. *IJCV*, 61(2):139–157, 2005.

[5] C. Broit. *Optimal Registration of Deformed Images*. PhD thesis, Computer and Information Science, University of Pensylvania, 1981.

[6] T. Chan and L. Vese. Active Contours Without Edges. *IEEE Transactions on Image Processing*, 10(2):266–277, 2001.

[7] Y. Chen, H. Thiruvenkadam, K. Gopinath, and R. Brigg. Image Registration Using the Mumford-Shah Functional and Shape Information. *World Multiconference on Systems, Cybernetics and Informatics*, pages 580–583, 2002.

[8] Y. Chen, H. Thiruvenkadam, H. Tagare, F. Huang, and D. Wilson. On the Incorporation of Shape Priors in Geometric Active Contours. *IEEE Workshop on Variational and Level Set Methods*, pages 145–152, 2001.

[9] G.E. Christensen. *Deformable Shape Models for Anatomy*. PhD thesis, Sever Institute of Technology, Washington University, 1994.

[10] G.E. Christensen, R.D. Rabbitt, and M.I. Miller. Deformable Templates Using Large Deformation Kinematics. *IEEE Transactions on Image Processing*, 5(10):1435–1447, 1996.

[11] P.-G. Ciarlet. *Elasticité Tridimensionnelle*. Masson, 1985.

[12] M.P. Do Carmo. *Differential Geometry of Curves and Surfaces*. Prentice-Hall, 1976.

[13] M. Droske and M. Rumpf. A variational approach to non-rigid morphological registration. *SIAM Appl. Math.*, 64(2):668–687, 2004.

[14] V. Duay, N. Houhou, and J.-P. Thiran. Atlas-based segmentation of medical images locally constrained by level sets. *ICIP 2005*, 2, 2005.

[15] B. Fischer and J. Modersitzki. Fast Diffusion Registration. *AMS Contemporary Mathematics, Inverse Problems, Image Analysis, and Medical Imaging*, 313:117–129, 2002.

[16] B. Fischer and J. Modersitzki. Curvature based image registration. *JMIV*, 18(1):81–85, 2003.

[17] B. Fischer and J. Modersitzki. A Unified Approach to Fast Image Registration and a New Curvature Based Registration Technique. *Linear Algebra and its applications, 380*, 23(7):107–124, 2004.

[18] E. Haber and J. Modersitzki. Numerical methods for volume preserving image registration. *Inverse problems, Institute of Physics Publishing*, 20(5):1621–1638, 2004.

[19] E. Haber and J. Modersitzki. Image Registration with Guaranteed Displacement Regularity. *International Journal of Computer Vision*, 71(3):361–372, 2007.

[20] X. Han, C. Xu, U. Braga-Neto, and J.L. Prince. Topology Correction in Brain Cortex Segmentation Using a Multiscale, Graph-Based Algorithm. *IEEE Transactions on Medical Imaging*, 21(2):109–121, 2002.

[21] X. Han, C. Xu, and J.L. Prince. A Topology Preserving Level Set Method for Geometric Deformable Models. *IEEE Transactions on Pattern Analysis and Machine Intelligence*, 25(6):755–768, 2003.

[22] K. P. Horn and B.G. Schunck. Determining Optical Flow. *Artificial Intelligence*, 17:185–203, 1981.

[23] H. Le Dret and A. Raoult. Enveloppe quasi-convexe de la densité d'eńergie de saint venant-kirchhoff. *C.R.A.S. I Maths.*, 318:93–98, 1994.

[24] C. Le Guyader and L. Vese. Self-repelling snakes for topology-preserving segmentation models. *to appear in IEEE Transactions on Image Processing*, 2008.

[25] A. Leow, M.-C. Chiang, H. Protas, P. Thompson, L. Vese, and H. S. C. Huang. Linear and Non-Linear Geometric Object Matching with implicit Representation. *Proceedings of the 17th International Conference on Pattern Recognition*, 3:710–713, 2004.

[26] W.-H. Liao, A. Khuu, M. Bergsneider, L. Vese, Huang S.-C., and S. Osher. From Landmark Matching to Shape and Open Curve Matching: A Level Set Approach. *UCLA CAM Report 02-59*, 2002.

[27] W.-H. Liao, H. Protas, M. Bergsneider, L. Vese, Huang S.-C., and S. Osher. A New Framework for Object Warping: A Semi-Lagrangian Level Set Approach. *Proceedings of the 2003 IEEE International Conference on Image Processing*, 2003.

[28] W.-H. Liao, C.-L. Yu, M. Bergsneider, L. Vese, and Huang S.-C. A New Framework of Quantifying Differences Between Images by Matching Gradient Fields and Its Application to Image Blending. *Nuclear Science Symposium Conference Record, IEEE*, 2:1092–1096, 2002.

[29] N. A. Lord, J. Ho, B. C. Vemuri, and S. Eisenschenk. Simultaneous Registration and Parcellation of Bilateral Hippocampal Surface Pairs for Local Asymmetry Quantification. *IEEE Transactions on Medical Imaging*, 26(4):471–478, 2007.

[30] J.B. Maintz and M.A. Viergever. A Survey of Medical Image Registration. *Medical Image Analysis*, 2:1–36, 1998.

[31] M. Miller, A. Trouvé, and L. Younes. On the metrics and euler-lagrange equations of computational anatomy. *Annu. Rev. B. Eng.*, 4:375–405, 2002.

[32] J. Modesitzki. *Numerical Methods for Image Registration*. Oxford University Press, 2004.

[33] D. Mumford and J. Shah. Optimal approximation by piecewise smooth functions and associated variational problems. *Commun. Pure Appl. Math.*, 42:577–685, 1989.

[34] P. V. Negrón Marrero. A numerical method for detecting singular minimizers of multidimensional problems in nonlinear elasticity. *Numerische Mathematik*, 58:135–144, 1990.

[35] S. Osher and R. Fedkiw. *Level Set Methods and Dynamic Implicit Surfaces.* Springer Verlag, 2003.

[36] S. Osher and N. Paragios. *Geometric Level Set Methods in Imaging, Vision, and Graphics.* Springer Verlag, 2003.

[37] S. Osher and J.A. Sethian. Fronts propagation with curvature dependent speed : Algorithms based on Hamilton-Jacobi formulations. *Journal of Computational Physics*, 79, 1988.

[38] P. Pedregal. *Variational methods in nonlinear elasticity.* SIAM, 2000.

[39] R.D. Rabbitt, J.A. Weiss, G.E. Christensen, and M.I. Miller. Mapping of hyperelastic deformable templates using the finite element method. *Proceedings SPIE*, 2573:252–265, 1995.

[40] Y. Rouchdy, J. Pousin, J. Schaerer, and P. Clarysse. A nonlinear elastic deformable template for soft structure segmentation: application to the heart segmentation in MRI. *Inverse Problems*, 23:1017–1035, 2007.

[41] J.A. Sethian. A Fast Marching Level Set Method for Monotonically Advancing fronts. *submitted for publication: Proceedings of the National Academy of Sciences*, 1995.

[42] J.A. Sethian. *Level Set Methods and Fast Marching Methods: Evolving interfaces in Computational Geometry, Fluid Mechanics, Computer Vision and Material Science.* Cambridge University Press, Londres, 1999.

[43] J.A. Sethian. Evolution, Implementation and Application of Level Set and Fast Marching Methods for Advancing Fronts. *Journal of Computational Physics*, 169(2):503–555, 2001.

[44] P. Smereka. Spiral crystal growth. *Physica D*, 138:282–301, 2000.

[45] G. Sundaramoorthi and A. Yezzi. Global regularizing flows with topology preservation for active contours and polygons. *IEEE Transactions on Image Processing*, 16(3):803–812, 2007.

[46] G.B. Unal and G.G. Slabaugh. Coupled pdes for non-rigid registration and segmentation. *CVPR*, pages 168–175, 2004.

[47] B. Vemuri and Y. Chen. Joint image registration and segmentation. *in Geometric Level Set Methods (S. Osher, N. Paragios, eds.)*, pages 251–269, 2003.

[48] B. Vemuri, J. Ye, Y. Chen, and C. Leonard. A level-set based approach to image registration. *IEEE Workshop on Mathematical Methods in Biomedical Image Analysis*, pages 86–93, 2000.

[49] B. Vemuri, J. Ye, Y. Chen, and C. Leonard. Image Registration via level-set motion: Applications to atlas-based segmentation. *Medical Image Analysis*, 7(1):1–20, 2003.

[50] L. Vese and T. Chan. A Multiphase Level Set Framework for Image Segmentation Using the Mumford and Shah Model. *International Journal of Computer Vision*, 50(3):271–293, 2002.

[51] F. Wang and B.C. Vemuri. Simultaneous registration and segmentation of anatomical structures from brain mri. *MICCAI*, pages 17–25, 2005.

[52] C. Xiaohua, J.M. Brady, and D. Rueckert. Simultaneous segmentation and registration of medical images. *MICCAI*, pages 663–670, 2004.

[53] C. Xu and J. Prince. Snakes, shapes, and gradient vector flow. *IEEE TIP*, 7:359–369, 1998.

[54] I. Yanovsky, P.M. Thompson, S. Osher, and A.D. Leow. Topology Preserving Log-Unbiased Nonlinear Image Registration: Theory and Implementation. *Computer Vision and Pattern Recognition, 2007. CVPR '07. IEEE Conference on*, 2007.

[55] A. Yezzi, L. Zollei, and T. Kapur. A variational framework for joint segmentation and registration. *IEEE-MMBIA*, pages 44–51, 2001.

Figure 4: On top, the boundary of the ellipse (zero level set of Φ_0) superimposed on the reference image, on the bottom, the topology-preserving segmentation of the two disks.
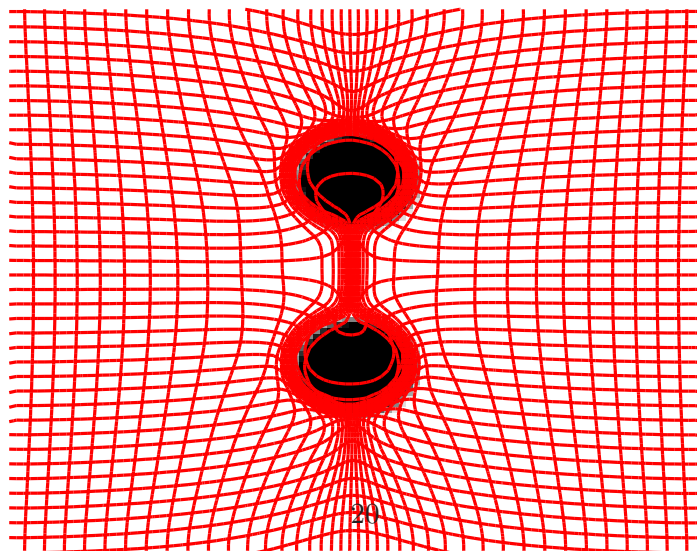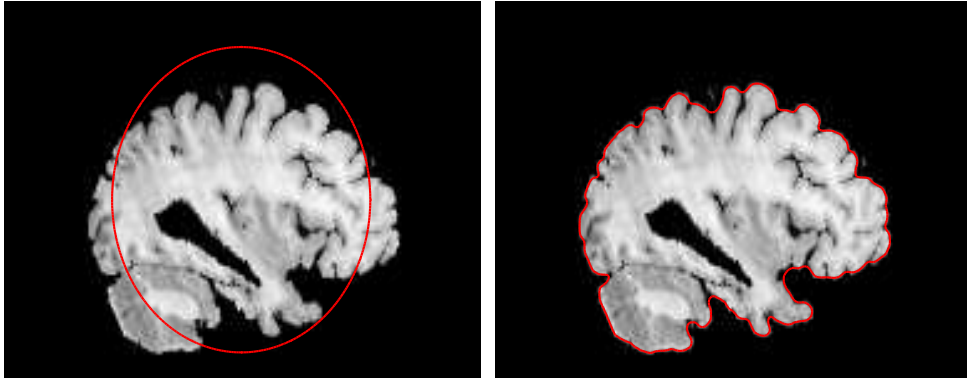
Figure 6: On the left, the boundary of the disk (zero level set of Φ_0) superimposed on the reference image, on the right, the segmentation of the slice of the brain.
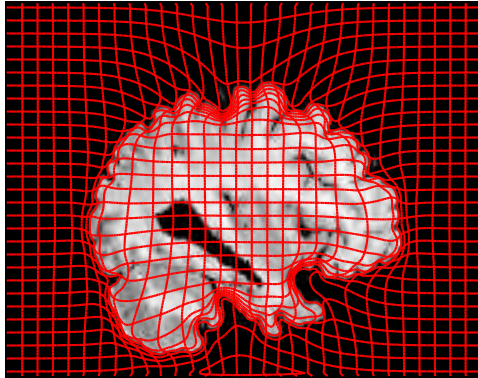
Figure 7: Deformed grid using nonlinear elasticity regularization. The parameters are: $\Delta t = 0.01$, Lamé coefficients $\lambda = 0$ and $\mu = 1000$, $\alpha = 20000$.